International Journal of Energy, Information and Communications
Vol.5, Issue 2 (2014), pp.13-34
http://dx.doi.org/10.14257/ijeic.2014.5.2.02

Broadband Radio Access Network Channel Identification and Downlink MC-CDMA Equalization

M. Zidane[1], S. Safi[2], M. Sabri[1], A. Boumezzough[3] and M. Frikel[4]

[1]*Department of Physics, Faculty of Sciences and technology, Sultan Moulay Slimane University, Beni Mellal, Morocco*
[2] *Department of Mathematics and Informatics, Polydisciplinary Faculty, Sultan Moulay Slimane University, Beni Mellal, Morocco*
[3] *Department of Physics, Polydisciplinary Faculty, Sultan Moulay Slimane University, Beni Mellal, Morocco*
[4] *GREYC laboratory, ENSICAEN School, Caen University, France*

zidane.ilco@gmail.com

Abstract

In this paper we propose a new algorithm based on third order cumulants, for MultiCarrier Code Division Multiple Access (MC-CDMA) system equalization. In order to test its efficiency, we have compared with the (CUM-AZ) algorithm proposed in the literature, for that we considered five practical frequency-selective fading channels, called Broadband Radio Access Network (BRAN A, BRAN B, BRAN C, BRAN D, and BRAN E), normalized for (MC-CDMA) system, excited by non-Gaussian sequences. In the part of (MC-CDMA), we use the zero forcing (ZF) and the minimum mean square error (MMSE) equalizers techniques after the channel identification to correct the channel's distortion. The simulation results, in noisy environment and for different signal to noise ratio (SNR), are presented to illustrate the performance of the proposed algorithm.

Keywords: *Blind identification, equalization, higher order cumulants, MC-CDMA system*

1. Introduction

During recent years, finite impulse response system identifcation based on Higher Order Cumulants (HOC) of system output, has increasingly been emphasized [1, 2, 3]. In the literature we have important results, established that blind identification of finite impulse response (FIR) single-input single-output (SISO) communication channels is possible only from the output second order statistics of the observed sequences [1]. But these approaches are sufficient only to identify Gaussian processes with minimal phase [2-4]. Moreover, the system to be identified has no minimum phase, excited by non Gaussian distribution input, and is contaminated by a Gaussian noise [2, 3] where the autocorrelation function (second order statistics) does not allow identifying the system correctly [2-4]. To overcome these problems, another approach was proposed by several authors [5-9, 11, 12, 13].This approach allow the resolution of the insoluble problems using the second order statistics.

In this paper, we will consider the problem of the identification of the Broadband Radio Access Network Channel such as BRAN A, B, C, D and E, normalized by the European Telecommunications Standards Institute (ETSI) [14] and [15], and downlink MC-CDMA Equalization. The principle of MC-CDMA transmits a data symbol of a user simultaneously on several narrowband sub-channels. These sub-channels are multiplied by the chips of the

ISSN: 2093-9655 IJEIC

user-specific spreading code, Multi-carrier modulation is realized by using the low complex OFDM operation. In most wireless environments, there are many obstacles in the channels, such as buildings, mountains and walls between the transmitter and the receiver. Reflections from these obstacles cause many different propagation paths. The problem encountered in communication is the synchronization between the transmitter and the receiver, due to the echoes and reflection between the transmitter and the receiver. Synchronization errors cause loss of orthogonality among sub-carriers and considerably degrade the performance especially when large number of subcarriers presents [19].

In this contribution, we propose an algorithm based, only, on third order cumulants. In order to test its efficiency, we have compared with the Antari, *et al.*, algorithm [6, 17]. The simulation results show that the bit error rate (BER) performances of the downlink MC-CDMA systems, using proposed algorithm (Algo3ZS) is more accurate compared with the results obtained with the Antari, *et al.*, (CUM_AZ) algorithm.

2. Problem Statement

The Broadband Radio Access Network channel output is modeled as the output of a *FIR* system that is excited by an unobservable input and is corrupted at its output by an additive white Gaussian noise (Figure 1).

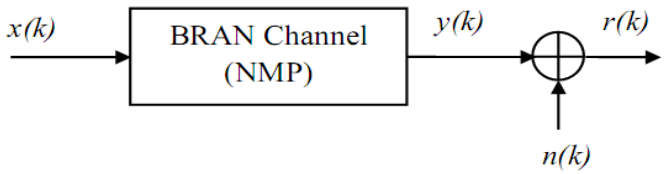

Figure 1. Channel model

The completely blind channel identification problem is to estimate h_q based only on the received signal $r(k)$ and without any knowledge of the energy of the transmitted data $x(k)$ nor the energy of noise.

The output time series is described by

Noise free case:

$$y(k) = \sum_{i=1}^{q} x(i)h(k-i). \quad (1)$$

With noise:

$$r(k) = y(k) + n(k). \quad (2)$$

The principal assumptions made on the model can be presented as follows: The input sequence, $\{x(k)\}$, is independent and identically distributed (i.i.d) zero mean, and non-Gaussian. The system is causal truncated, i.e. $h(k) = 0$ for $i < 0$ and $i > q$, where $h(0) = 1$. The system order q is known. The measurement noise sequence $\{n(k)\}$ is assumed zero mean, Gaussian and independent of $\{x(k)\}$ with unknown variance.

3. Proposed Algorithm: Algo3ZS

The m^{th} order cumulants of the {y(n)} can be expressed as a function of impulse response coefficients {h(i)} as follows [5-7, 16, 17]:

$$C_{my}(t_1, \dots, t_{m-1}) = \gamma_{mx} \sum_{i=0}^{q} h(i)h(i+t_1) \dots h(i+t_{m-1}), \quad (3)$$

where γ_{mx} represents the m^{th} order cumulants of the excitation signal $\{x(i)\}$ at origin.

If m = 2, Eq. (3) yield to

$$C_{2y}(t) = \gamma_{2x} \sum_{i=0}^{q} h(i)h(i+t). \quad (4)$$

The same, if m = 3, Eq. (3) becomes

$$C_{3y}(t_1, t_2) = \gamma_{3x} \sum_{i=0}^{q} h(i)h(i+t_1)\, h(i+t_2). \quad (5)$$

The Fourier transforms of the 2nd and 3rd order cumulants are given respectively by the following equations:

$$S_{2y}(\omega) = TF\{C_{2y}(t)\} = \gamma_{2x} \sum_{i=0}^{q} \sum_{t=-\infty}^{+\infty} h(i)h(i+t)\, exp(-j\omega t) \; = \gamma_{2x} H(-\omega)H(\omega), \quad (6)$$

$$S_{3y}(\omega_1, \omega_2) = TF\{C_{3y}(t_1, t_2)\} = \gamma_{3x} H(-\omega_1 - \omega_2)H(\omega_1)H(\omega_2). \quad (7)$$

If we suppose that $\omega = (\omega_1 + \omega_2)$, Eq. (6) reduces:

$$S_{2y}(\omega_1 + \omega_2) = \gamma_{2x} H(-\omega_1 - \omega_2)H(\omega_1 + \omega_2). \quad (8)$$

Then, from Eqs. (7) and (8) we obtain the following equation

$$S_{3y}(\omega_1, \omega_2)H(\omega_1 + \omega_2) = \mu H(\omega_1)H(\omega_2)S_{2y}(\omega_1 + \omega_2), \quad (9)$$

with $\mu = \frac{\gamma_{3x}}{\gamma_{2x}}$

The inverse Fourier transform of Eq. (9) demonstrates that the 3rd order cumulants, the second order statistics (autocorrelation function) and the impulse response channel parameters are combined by the following equation:

$$\sum_{i=0}^{q} C_{3y}(t_1 - i, t_2 - i)h(i) = \mu \sum_{i=0}^{q} h(i)h(t_2 - t_1 + i)\, C_{2y}(t_1 - i) \quad (10)$$

If we use the ACF property of the stationary process such as $C_{2y}(t) \neq 0$ only for $-q \leq t \leq q$ and vanishes elsewhere.

If we suppose that $t_1 = 2q$ the Eq. (10) reduces:

$$\sum_{i=0}^{q} C_{3y}(2q - i, t_2 - i)h(i) = \mu h(q)h(t_2 - q)\, C_{2y}(q), \quad (11)$$

else, if we suppose that $t_2 = 2q$, Eq. (11) will become

$$C_{3y}(q,q)h(q) = \mu h^2(q) C_{2y}(q). \tag{12}$$

Using Eqs. (11) and (12) we obtain the following relation :

$$\sum_{i=0}^{q} C_{3y}(2q-i, t_2-i)h(i) = C_{3y}(q,q)\, h(t_2-q), \tag{13}$$

else, if we suppose that the system is causal, *i.e.*, $h(i) = 0$ if $i < 0$. So, for $t_2 = q,\ldots,2q$, the system of Eq. (13) can be written in matrix form as:

$$\begin{pmatrix} C_{3y}(2q-1,q-1) & \cdots & C_{3y}(q,0) \\ C_{3y}(2q-1,q)-\alpha & \cdots & C_{3y}(q,1) \\ \vdots & \ddots & \vdots \\ C_{3y}(2q-1,2q-1) & \cdots & C_{3y}(q,q)-\alpha \end{pmatrix} \times \begin{pmatrix} h(1) \\ \vdots \\ h(i) \\ \vdots \\ h(q) \end{pmatrix} = \begin{pmatrix} \alpha - C_{3y}(2q,q) \\ -C_{3y}(2q,q+1) \\ \vdots \\ -C_{3y}(2q,2q) \end{pmatrix} \tag{14}$$

where $\alpha = C_{3y}(q,q)$

Or in more compact form, the Eq. (14) can be written as follows:

$$Mh = d, \tag{15}$$

where M is the matrix of size $(q+1) \times (q)$ elements, $h(i)$ is a column vector constituted by the unknown impulse response parameters $h(i) : i = 1,\ldots,q$ and d is a column vector of size $(q+1)$ as indicated in the Eq. (15).

The least squares (LS) solution of the system of Eq. (15):

$$\hat{h} = (M^T M)^{-1} M^T d \tag{16}$$

4. Antari, *et al.*, Algorithm: CUM_AZ [6, 17]

Antari, *et al.*, [6, 17] demonstrate that the coefficients $h(i)$ for an *FIR* system can be obtained by the relationship, based on fourth order cumulants following:

$$\sum_{i=0}^{q} C_{4y}(2q-i, t_2-i, 2q-i)h(i) = \beta h(t_2-q), \tag{17}$$

with $\beta = \left(\frac{C_{4y}(q,q,q)}{C_{4y}(q,q,0)}\right)^2 C_{3y}(q,0,0)$,

with $t_2 = q,\ldots,2q$

In the same manner, in more compact form, the Eq. (17) can be written as follows:

$$Mh = d. \tag{18}$$

The least squares solution, will be written under the following form

$$\hat{h} = (M^T M)^{-1} M^T d. \tag{19}$$

5. Equalization of MC-CDMA system

The multicarrier code division multiple access (MC-CDMA) system is based on the combination of code division multiple access (CDMA) and orthogonal frequency division multiplexing (OFDM) which is potentially robust to channel frequency selectivity.

5.1.M C-CDMA Transmitter

In the MC-CDMA modulator the complex symbol a_i of each user i is, first, multiplied by each chip $c_{i,k}$ of spreading code, and then applied to the modulator of multicarriers. The MC-CDMA emitted signal is given by

$$\mathrm{x(t)} = \frac{1}{\sqrt{\mathrm{N_p}}} \sum_{\mathrm{k=0}}^{\mathrm{N_{p-1}}} \mathrm{a_i c_{i,k} e^{2jf_k t}} \tag{20}$$

where $\mathrm{f_k} = \mathrm{f_0} + {}^{\mathrm{k}}/_{\mathrm{T_c}}$, $\mathrm{N_u}$ is the user number and $\mathrm{N_p}$ is the number of subcarriers, and we consider $L_c = \mathrm{N_p}$.

We suppose that the channel is time invariant and it's impulse response is characterized by P paths of magnitudes β_p and phases θ_p. So the impulse response is given by

$$h(\tau) = \sum_{p=0}^{P-1} \beta_p e^{j\theta_p}\, \delta(\tau - \tau_p) \tag{21}$$

5.2.MC-CDMA Receiver

The downlink received MC-CDMA signal at the input receiver is given by the following equation [5]:

$$r(t) = \frac{1}{\sqrt{N_p}} \sum_{p=0}^{P-1} \sum_{k=0}^{N_p-1} \sum_{i=0}^{N_u-1} R\left\{\beta_p e^{j\theta} a_i c_{i,k} e^{2j\pi\left(f_0 + {}^{k}/_{T_c}\right)(t-\tau_p)}\right\} + n(t), \tag{22}$$

where $n(t)$ is an additive white Gaussian noise.

The equalization goal, is to obtain a good estimation of the symbol a_i. At the reception, we demodulate the signal according the N_p subcarriers, and then we multiply the received sequence by the code of the user. Figure 2 explains the single user-detection principle.

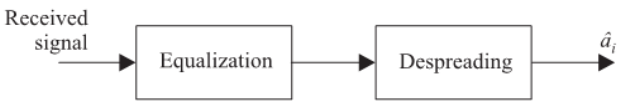

Figure 2. Principle of the single user-detection

After the equalization and the spreading operation, the estimation $\hat{a_i}$ of the emitted user symbol a_i, of the i^{th} user can be written by the following equation

$$\widehat{a_i} = \sum_{q=0}^{N_u-1}\sum_{k=0}^{N_p-1} c_{i,k}\left(g_k h_k c_{q,k} a_q + g_k n_k\right) = \underbrace{\sum_{k=0}^{N_p-1} c_{i,k}^2 g_k h_k a_i}_{I} + \underbrace{\sum_{q=0}^{N_u-1}\sum_{k=0}^{N_p-1} c_{i,k} c_{q,k}\, g_k h_k a_q}_{II\ (q\neq i)} + \underbrace{\sum_{k=0}^{N_p-1} c_{i,k}^2\, g_k n_k}_{III}, \quad (23)$$

where the term I, II and III of Eq. (23) are, respectively, the signal of the considered user, a signals of the others users (multiple access interferences) and the noise pondered by the equalization coeffcient and by spreading code of the chip.

5.3. Equalization for MC-CDMA

5.3.1 Zero forcing (ZF)

The principle of the ZF, is to completely cancel the distortions brought by the channel. The gain factor of the ZF equalizer, is given by the equation:

$$g_k = \frac{1}{|h_k|} \quad (24)$$

By that manner, each symbol is multiplied by a unit magnitude. So, the estimated received symbol, $\widehat{a_i}$ of symbol a_i of the user i is described by:

$$\widehat{a_i} = \underbrace{\sum_{k=0}^{N_p-1} c_{i,k}^2 a_i}_{I} + \underbrace{\sum_{q=0}^{N_u-1}\sum_{k=0}^{N_p-1} c_{i,k} c_{q,k}\, a_q}_{II\ (q\neq i)} + \underbrace{\sum_{k=0}^{N_p-1} c_{i,k}\frac{1}{h_k} n_k}_{III} \quad (25)$$

If we suppose that the spreading code are orthogonal, i.e.,

$$\sum_{k=0}^{N_p-1} c_{i,k}\, c_{q,k} = 0\ \forall\ i \neq q \quad (26)$$

Eq. (25) will become

$$\widehat{a_i} = \sum_{k=0}^{N_p-1} c_{i,k}^2 a_i + \sum_{k=0}^{N_p-1} c_{i,k}\frac{1}{h_k} n_k \quad (27)$$

5.3.2Minimum Mean Square Error (MMSE)

The MMSE techniques minimize the mean square error for each subcarrier k between the transmitted signal x_k and the output detection

$$\varepsilon[|\varepsilon|^2] = \varepsilon[|\mathrm{x_k} - \mathrm{g_k r_k}|^2]. \quad (28)$$

The minimization of the function $\varepsilon[|\varepsilon|^2]$, gives us the optimal equalizer coefficient, under the minimization of the mean square error criterion, of each subcarrier as :

$$g_k = \frac{h_k^*}{|h_k|^2 + \frac{1}{\gamma_k}}, \tag{29}$$

where $\gamma_k = \frac{E[|r_k h_k|^2]}{E[|n_k|^2]}$.

$$\widehat{a_i} = \underbrace{\sum_{k=0}^{N_p-1} c_{i,k}^2 \frac{|h_k|^2}{|h_k|^2 + \frac{1}{\gamma_k}} a_i}_{I} + \underbrace{\sum_{q=0}^{N_u-1} \sum_{k=0}^{N_p-1} c_{i,k} c_{q,k} \frac{|h_k|^2}{|h_k|^2 + \frac{1}{\gamma_k}} a_q}_{II \quad (q \neq i)} + \underbrace{\sum_{k=0}^{N_p-1} c_{i,k}^2 \frac{h_k^*}{|h_k|^2 + \frac{1}{\gamma_k}} n_k}_{III} \tag{30}$$

The same, if we suppose that the spreading code are orthogonal, Eq. (30) will reduces:

$$\widehat{a_i} = \sum_{k=0}^{N_p-1} c_{i,k}^2 \frac{|h_k|^2}{|h_k|^2 + \frac{1}{\gamma_k}} a_i + \sum_{k=0}^{N_p-1} c_{i,k} \frac{h_k^*}{|h_k|^2 + \frac{1}{\gamma_k}} n_k. \tag{31}$$

6. Simulation Results

In this section we consider the BRAN A, B, C, D, and E model representing the fading radio channels, the data corresponding to this model are measured for multicarrier code division multiple access (MC-CDMA) systems. The following equation describes the impulse response $h(k)$ of BRAN radio channel:

$$h(k) = \sum_{i=0}^{N_T} A_i \, \delta(k - \tau_i). \tag{32}$$

Thus, the BRAN channels is constituted by $N_T = 18$ parameters and seeing that the latest parameters are very small. So, in order to estimates the parameters constituting the BRAN channels impulse response, we have taking the following procedure:

- We decompose the BRAN channel impulse response into four sub-channel as follow:

$$\mathrm{h(k)} = \sum_{\mathrm{j}=1}^{3} \mathrm{h_j\,(k)}. \tag{33}$$

- We estimate the parameters of each sub-channel independently, we add all sub channel parameters, to construct the full BRAN channels impulse response.

6.1. Bran A radio channel

In Table 1 we have summarized the values corresponding the BRAN A radio channel impulse response

Table 1. Delay and magnitudes of 18 targets of BRAN A channel

$Delay\ \tau_i[ns]$	$Mag.A_i[dB]$	$Delay\ \tau_i[ns]$	$Mag.A_i[dB]$
0	0.0	90	-7.8
10	-0.9	110	-4.7
20	-1.7	140	-7.3
30	-2.6	170	-9.9
40	-3.5	200	-12.5
50	-4.3	240	-13.7
60	-5.2	290	-18
70	-6.1	340	-22.4
80	-6.9	390	-26.7

In time domain we have represented the BRAN A channel impulse response parameters using proposed algorithm (Algo3ZS), compared with the results obtained with the Antari, *et al.*, (CUM_AZ) algorithm (Figure 3).

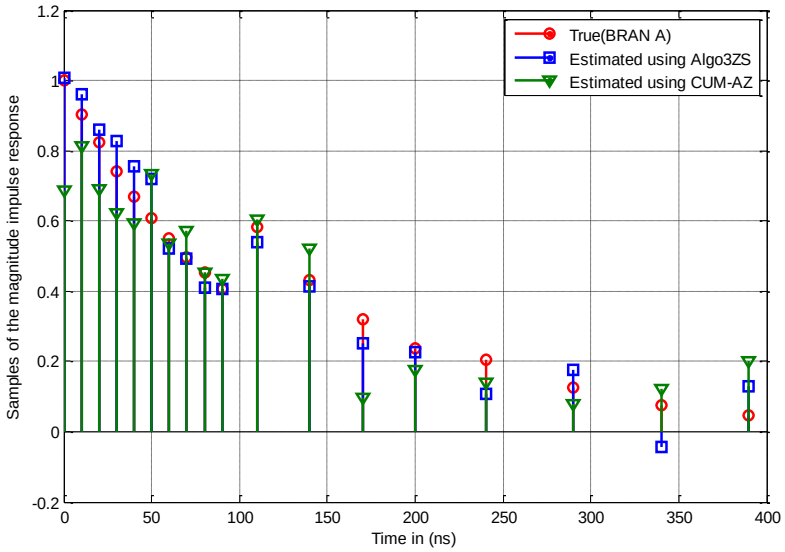

Figure 3. Estimated of the BRAN A channel impulse response, for an SNR = 16 dB and a data length N=4800

From the Figure 3 we ca can conclude that the estimated BRAN A channel impulse response are very closed to the true ones, than those obtained by the Antari, *et al.*, (CUM_AZ) principally for high data length (N = 4800), and for $SNR = 16\ dB$.

In the following figure (Figure 4) we have represented the estimated magnitude and phase of the impulse response BRAN A using all target, for an data length N = 4800 and *SNR=20 dB*, obtained using proposed algorithm (Algo3ZS), compared with the (CUM_AZ) algorithm.

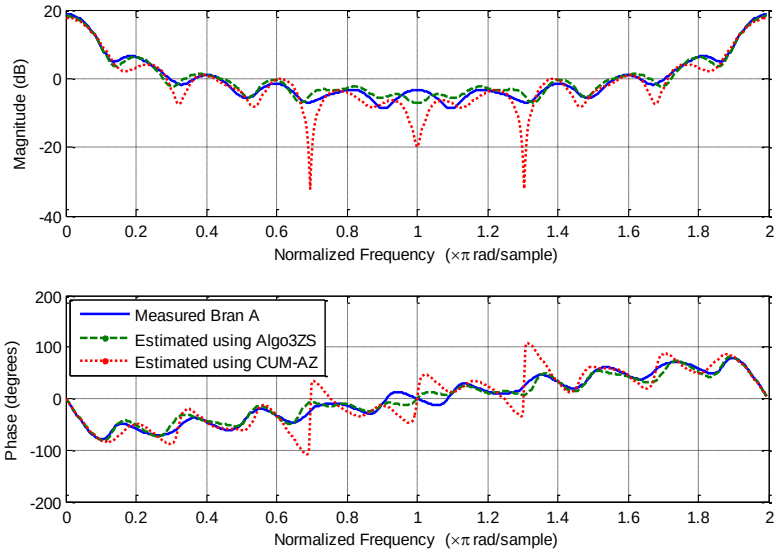

Figure 4. Estimated of the BRAN A channel impulse response using all target, for an SNR = 20 dB and a data length N=4800

From the Figure 4, we remark that the magnitude and phase estimations using proposed algorithm (Algo3ZS), have the same allure comparatively to the true ones, than those obtained by the Antari, *et al.*, (CUM_AZ) algorithm, we have a difference between the estimated and the measured ones.

6.2. Bran B radio channel

In Table 2 we have represented the values corresponding to the BRAN B radio channel impulse response.

Table 2. delay and magnitudes of 18 targets of bran B channel

Delay τ_i[ns]	Mag. A_i[dB]	Delay τ_i[ns]	Mag. A_i[dB]
0	−2.6	230	−5.6
10	−3.0	280	−7.7
20	−3.5	330	−9.9
30	−3.9	380	−12.1
50	0.0	430	−14.3
80	−1.3	490	−15.4
110	−2.6	560	−18.4
140	−3.9	640	−20.7
180	−3.4	730	−24.6

In time domain we have represented the BRAN B channel impulse response parameters using proposed algorithm (Algo3ZS), compared with the results obtained with the Antari, *et al.*, (CUM_AZ) algorithm (Figure 5).

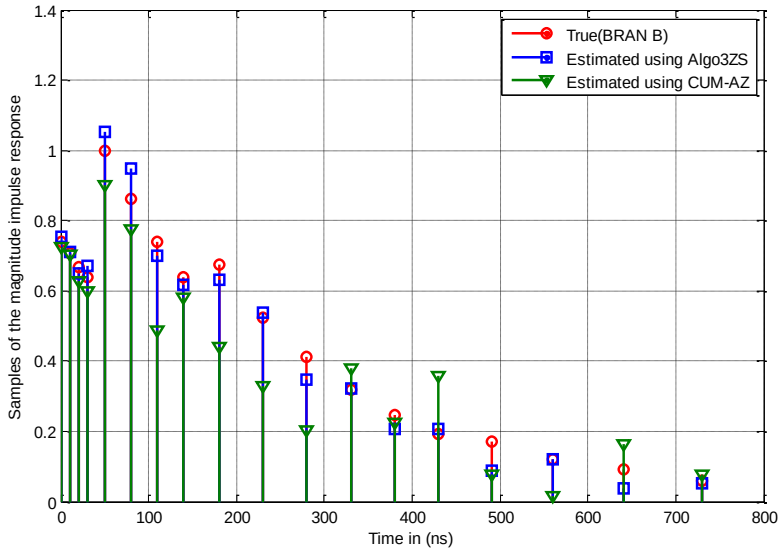

Figure 5. Estimated of the BRAN B channel impulse response, for an SNR = 16 dB and a data length N=4800

From Figure 5, we can conclude that the proposed algorithm (Algo3ZS) give us a good estimation for all parameters of BRAN B radio channel impulse response, compared with the results obtained by the (CUM_AZ) algorithm.

In the following figure (Figure 6) we have represented the estimated magnitude and phase of the impulse response BRAN B using all target, for an data length N = 4800 and *SNR=20 dB*, obtained using proposed algorithm (Algo3ZS), compared with the (CUM_AZ) algorithm.

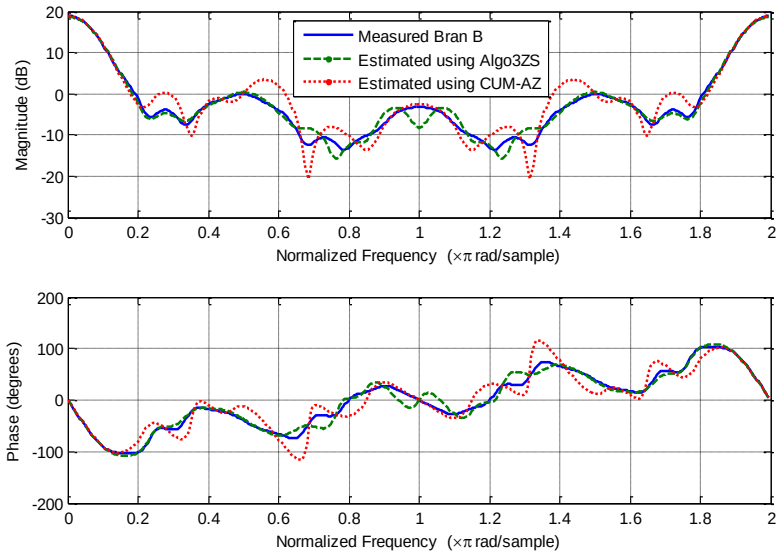

Figure 6. Estimated of the BRAN B channel impulse response using all target, for an SNR = 20 dB and a data length N=4800

From the Figure 6 we observe that the estimated magnitude and phase, using proposed algorithm (Algo3ZS) are the same allure and we have not more difference between the estimated and the true ones, than those obtained by the (CUM_AZ) algorithm we remark a difference between the estimated and the measured ones.

6.3. Bran C radio channel

In Table 3 we have represented the values corresponding to the BRAN C radio channel impulse response

Table 3. Delay and magnitudes of 18 targets of bran C channel

Delay τ_i[ns]	Mag. A_i[dB]	Delay τ_i[ns]	Mag. A_i[dB]
0	−3.3	230	−3.0
10	−3.6	280	−4.4
20	−3.9	330	−5.9
30	−4.2	400	−5.3
50	0.0	490	−7.9
80	−0.9	600	−9.4
110	−1.7	730	−13.2
140	−2.6	880	−16.3
180	−1.5	1050	−21.2

In time domain we have represented the BRAN C channel impulse response parameters using proposed algorithm (Algo3ZS), compared with the results obtained with the Antari, *et al.*, (CUM_AZ) algorithm (Figure 7).

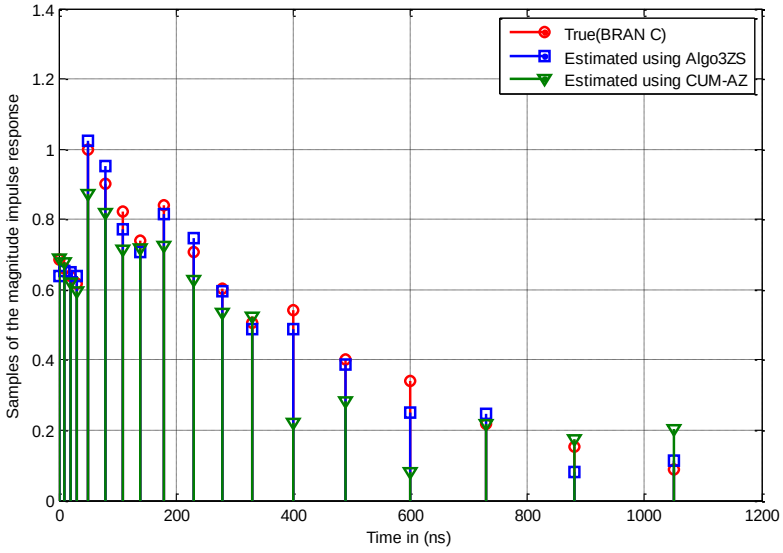

Figure 7. Estimated of the BRAN C channel impulse response, for an SNR = 16 dB and a data length N=4800

From the figure (Figure 7) we have approximately the same allure of the estimated and the true ones, using proposed algorithm (Algo3ZS), compared with the results obtained with the (CUM_AZ) algorithm we remark a difference between the estimated and the measured ones.

In the following figure (Figure 8) we have represented the estimated magnitude and phase of the impulse response BRAN C using all target, for an data length N = 4800 and *SNR=20 dB*, obtained using proposed algorithm (Algo3ZS), compared with the (CUM_AZ) algorithm.

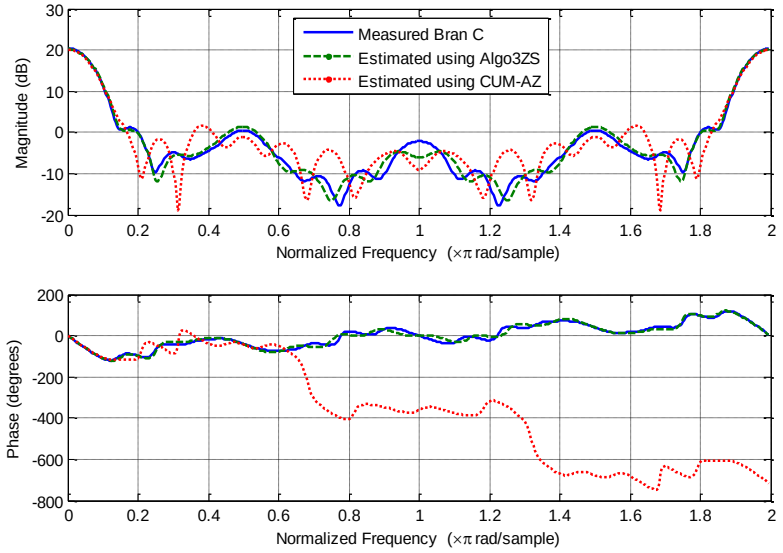

Figure 8. Estimated of the BRAN C channel impulse response using all target, for an SNR = 20 dB and a data length N=4800

From the Figure 8 we observe that the estimated magnitude will be more closed to the true ones using (Algo3ZS), but using (CUM_AZ) we remark a minor difference between the estimated magnitude and the measured ones. Now we have estimated the phase of BRAN C channel impulse response.We remak an apparent progress of the phase estimation, more closed to the true ones, using Algo3ZS, but using (CUM_AZ) we remark a more difference between the estimated phase and the measured ones.

1. Bran D radio channel

In Table 4 we have represented the values corresponding to the BRAN D radio channel impulse response.

Table 4. delay and magnitudes of 18 targets of bran D channel

Delay τ_i[ns]	Mag. A_i[dB]	Delay τ_i[ns]	Mag. A_i[dB]
0	0.0	230	−9.4
10	−10.0	280	−10.8
20	−10.3	330	−12.3
30	−10.6	400	−11.7
50	−6.4	490	−14.3
80	−7.2	600	−15.8
110	−8.1	730	−19.6
140	−9.0	880	−22.7
180	−7.9	1050	−27.6

In time domain we have represented the BRAN D channel impulse response parameters using proposed algorithm (Algo3ZS), compared with the results obtained with the Antari, *et al.*, (CUM_AZ) algorithm (Figure 9).

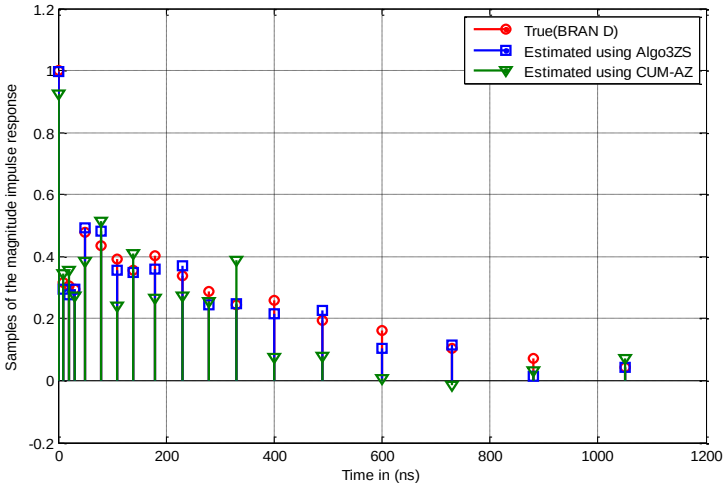

Figure 9. Estimated of the BRAN D channel impulse response, for an SNR = 16 dB and a data length N=4800

From Figure 9, we can conclude that the algorithm (Algo3ZS) give us a good estimation for all parameters of BRAN D radio channel impulse response, than those obtained by the (CUM_AZ) algorithm.

In the following figure (figure 10) we have represented the estimated magnitude and phase of the impulse response BRAN D using all target, for an data length N = 4800 and *SNR=16 dB*, obtained using proposed algorithm (Algo3ZS), compared with the (CUM_AZ) algorithm.

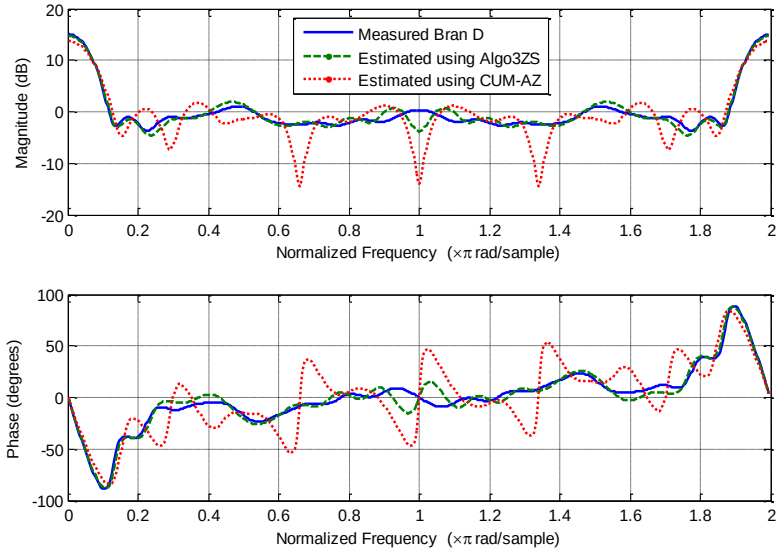

Figure 10. Estimated of the BRAN D channel impulse response using all target, for an SNR = 16 dB and a data length N=4800

From the Figure 10 we observe that the estimated magnitude and phase will be more closed to the true ones using (Algo3ZS), but using (CUM_AZ) we remark more difference between the estimated (magnitude and phase) and the measured ones.

2. Bran E radio channel

In Table 5 we have represented the values corresponding to the BRAN E radio channel impulse response.

Table 5. delay and magnitudes of 18 targets of bran E channel

Delay τ_i[ns]	Mag. A_i[dB]	Delay τ_i[ns]	Mag. A_i[dB]
0	−4.9	320	0.0
10	−5.1	430	−1.9
20	−5.2	560	−2.8
40	−0.8	710	−5.4
70	−1.3	880	−7.3
100	−1.9	1070	−10.6
140	−0.3	1280	−13.4
190	−1.2	1510	−17.4
240	−2.1	1760	−20.9

In time domain we have represented the BRAN E channel impulse response parameters using proposed algorithm (Algo3ZS), compared with the results obtained with the Antari et al (CUM_AZ) algorithm (Figure 11).

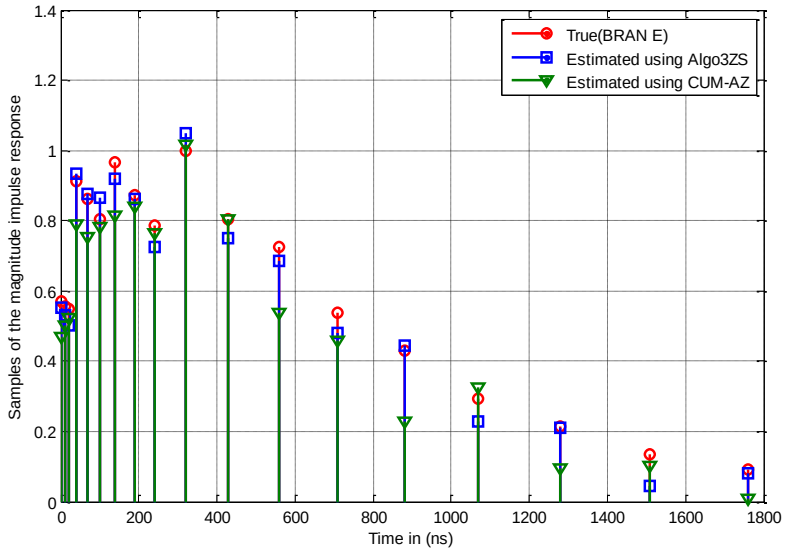

Figure 11. Estimated of the BRAN E channel impulse response, for an SNR = 16 dB and a data length N=4800

From the Figure 11, we remark that the estimated using proposed algorithm (Algo3ZS), have the same allure comparatively to the true ones, than those obtained by (CUM_AZ) algorithm, we have a minor difference between the estimated and the measured ones.

In the following figure (Figure 12) we have represented the estimated magnitude and phase of the impulse response BRAN E using all target, for an data length N = 4800 and *SNR=20 dB*, obtained using proposed algorithm (Algo3ZS), compared with the (CUM_AZ) algorithm.

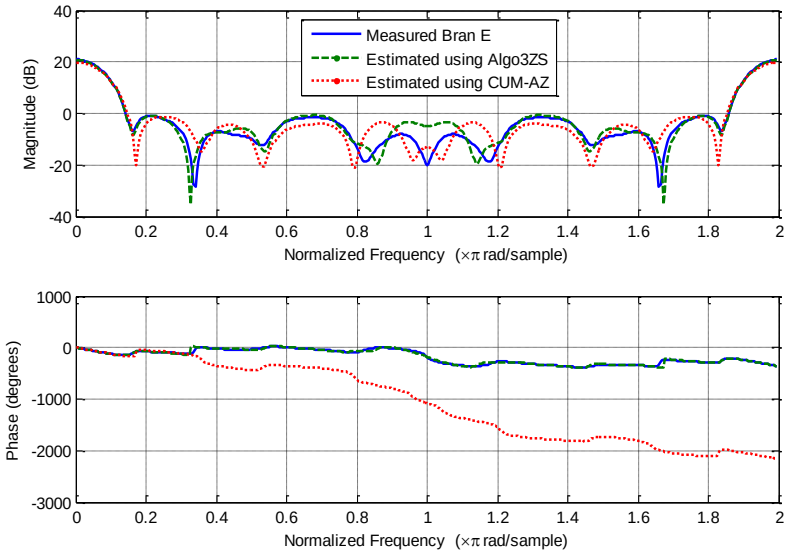

Figure 12. Estimated of the BRAN E channel impulse response using all target, for an SNR = 20 dB and a data length N=4800

From the Figure 12 we observe that the estimated phase, using proposed algorithm (Algo3ZS) are close to the true ones, than those obtained by the (CUM_AZ) algorithm we remark more difference between the estimated phase and the measured ones. This is because the BRAN E impulse response have more fluctuations.

7. Application: MC-CDMA system performance

In this section we used the Minimum Mean Square Error, (MMSE) and zero forcing (ZF) equalizers for MC-CDMA. The results are evaluated for different values of *SNR*.

7.1. ZF and MMSE Equalizers: Case of BRAN A Channel

In Figure 13, we represent the BER, obtained using the ZF equalizer, for different SNR, using proposed algorithm (Algo3ZS), compared with the (CUM_AZ) algorithm

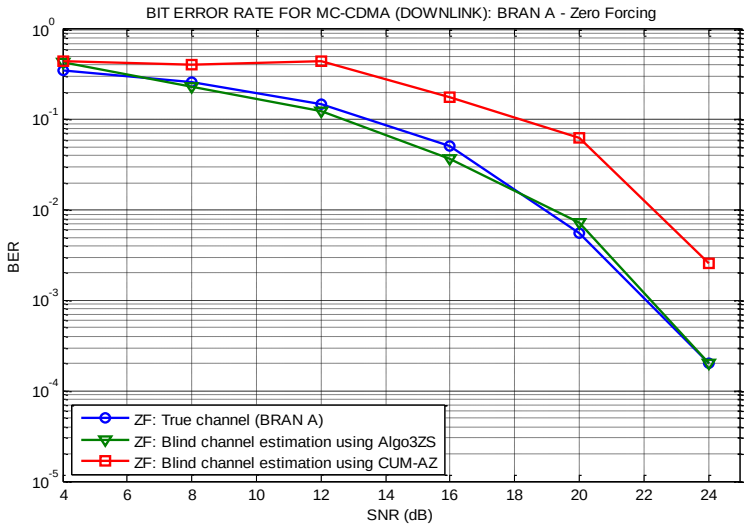

Figure 13. BER of the estimated and measured BRAN A channel using the ZF equalizer

Figure 14 represents the BER, obtained using MMSE equalizer, for different SNR, using proposed algorithm (Algo3ZS), compared with the (CUM_AZ) algorithm.

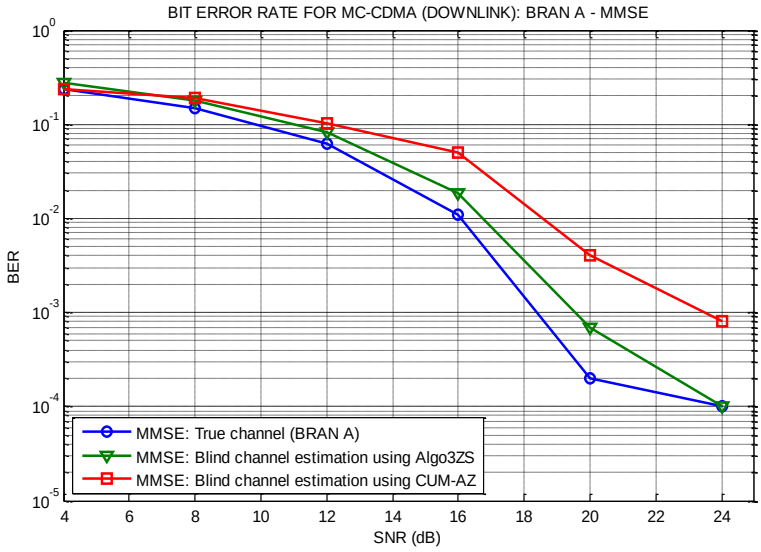

Figure 14. BER of the estimated and measured BRAN A channel using the MMSE equalizer

The BER simulation for different SNR, demonstrates that the estimated values by the (Algo3ZS) algorithm are more close to the measured value than those estimated by (CUM_AZ) algorithm for ZF and MMSE equalization. From the Figure 13 and 14, we conclude that: if the *SNR=24 dB* we have 1 bit error occurred when we receive 10^3 bit using (CUM_AZ), but using (Algo3ZS) we obtain only one bit error for 10^4 bit received.

7.2. ZF and MMSE Equalizers: Case of BRAN B Channel

In Figure 15, we represent the BER for different SNR, obtained using proposed algorithm (Algo3ZS), compared with the (CUM_AZ) algorithm, but the equalization is performed using the ZF equalizer.

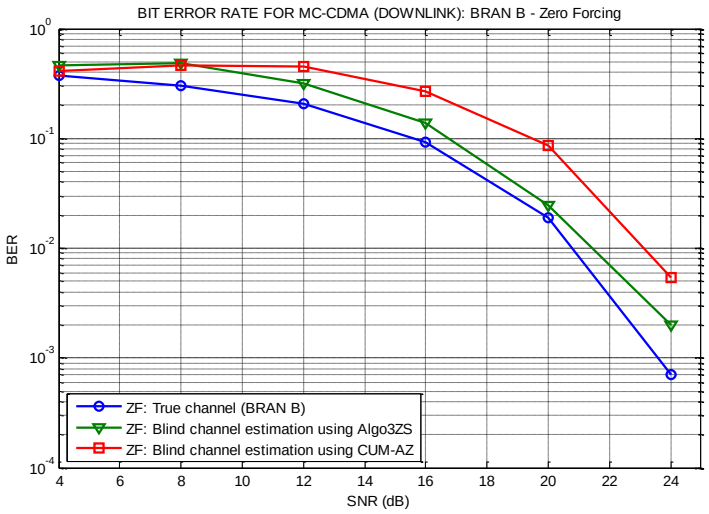

Figure 15. BER of the estimated and measured BRAN B channel using the ZF equalizer

From the Figure 15, we observe that the blind ZF equalization give us approximately the same results obtained by the measured BRAN B values using Algo3ZS, than those obtained by (CUM_AZ) algorithm, we have a difference between the estimated and the measured ones.

Using the MMSE equalizer we represents, Figure 16, the BER for different SNR, obtained using proposed algorithm (Algo3ZS), compared with the (CUM_AZ) algorithm.

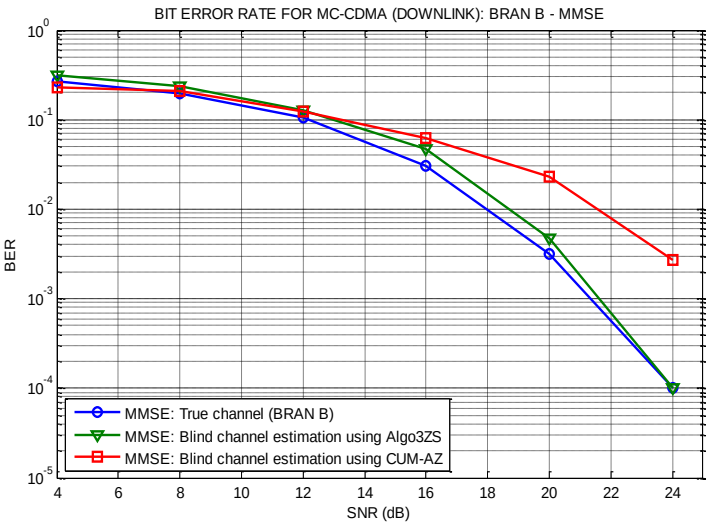

Figure 16. BER of the estimated and measured BRAN B channel using the MMSE equalizer

From the Figure 16, we remark that the MMSE equalization using proposed algorithm (Algo3ZS), have the same allure comparatively to the true ones, than those obtained by (CUM_AZ) algorithm, thus, if the *SNR=24 dB*, we observe that 1 bit error occurred when we receive, approximately, 10^3 bit with the (CUM_AZ), but using (Algo3ZS) we obtain only one bit error for 10^4 bit received.

7.3. ZF and MMSE Equalizers: Case of BRAN C Channel

In Figure 17, we represent, using the ZF equalizer technique, the BER for different SNR, obtained using proposed algorithm (Algo3ZS), compared with the (CUM_AZ) algorithm.

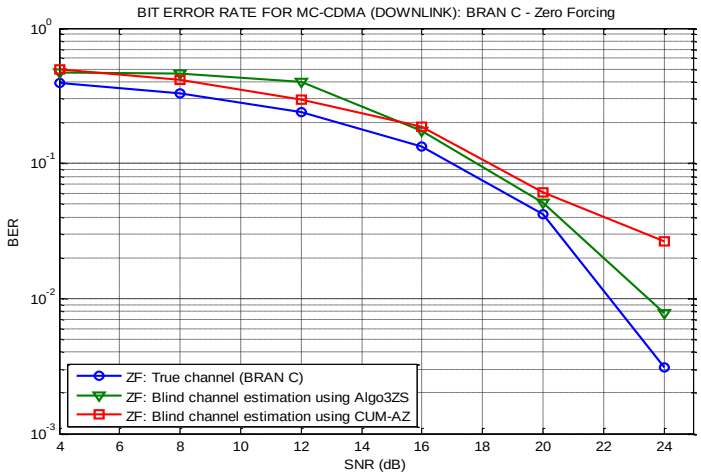

Figure 17. BER of the estimated and measured BRAN C channel using the ZF equalizer

Figure 18 represents the BER for different SNR, obtained using proposed algorithm (Algo3ZS), compared with the (CUM_AZ) algorithm, but the equalization is performed using the MMSE equalizer.

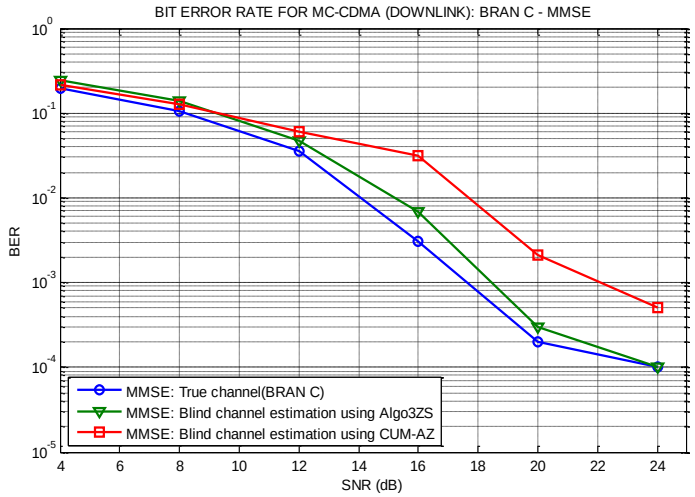

Figure 18. BER of the estimated and measured BRAN C channel using the MMSE equalizer

From Figure 18, we conclude that: if the SNR values are superior to 24 dB we have a BER than 10^{-4} with the (CUM_AZ), but using the (Algo3ZS) we have only the BER than 10^{-5}, principally if we use the MMSE equalizer.

7.4. ZF and MMSE Equalizers: Case of BRAN D Channel

In Figure 19, we represent the BER for different SNR, obtained using proposed algorithm (Algo3ZS), compared with the (CUM_AZ) algorithm, but the equalization is performed using the ZF equalizer.

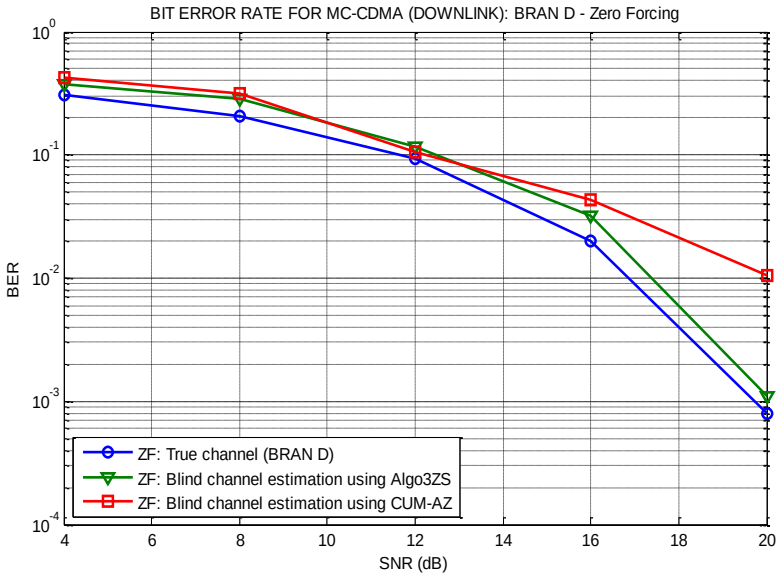

Figure 19. BER of the estimated and measured BRAN D channel using the ZF equalizer

Figure 19 demonstrates that the proposed algorithm (Algo3ZS) more accurate than those Antari et al (CUM_AZ), So, if the *SNR=20 dB*, we observe that 1 bit error occurred when we receive 10^2 bit with the (CUM_AZ), but using (Algo3ZS) we obtain only one bit error for 10^3 bit received.

Figure 20 represents the BER for different SNR, obtained using proposed algorithm (Algo3ZS), compared with the (CUM_AZ) algorithm, but the equalization exploiting the MMSE equalizer.

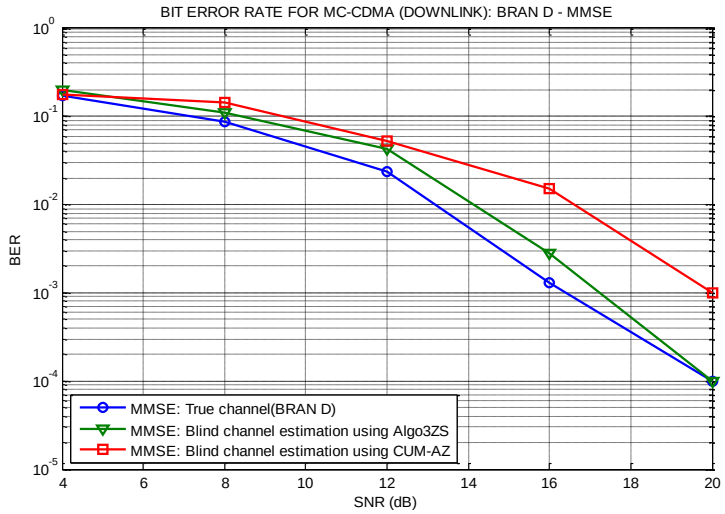

Figure 20. BER of the estimated and measured BRAN D channel using the MMSE equalizer

Figure 20 demonstrates clearly that the estimated values by the first algorithm (Algo3ZS) are more close to the measured value than those estimated by second algorithm (CUM_AZ), thus, if the *SNR=20 dB*, we observe that 1 bit error occurred when we receive 10^3 bit with the (CUM_AZ), but using (Algo3ZS) we obtain only one bit error for 10^4 bit received.

7.5. ZF and MMSE Equalizers: Case of BRAN E Channel

In Figure 21, we represent the BER for different SNR, obtained using proposed algorithm (Algo3ZS), compared with the (CUM_AZ) algorithm, but the equalization is performed using the ZF equalizer.

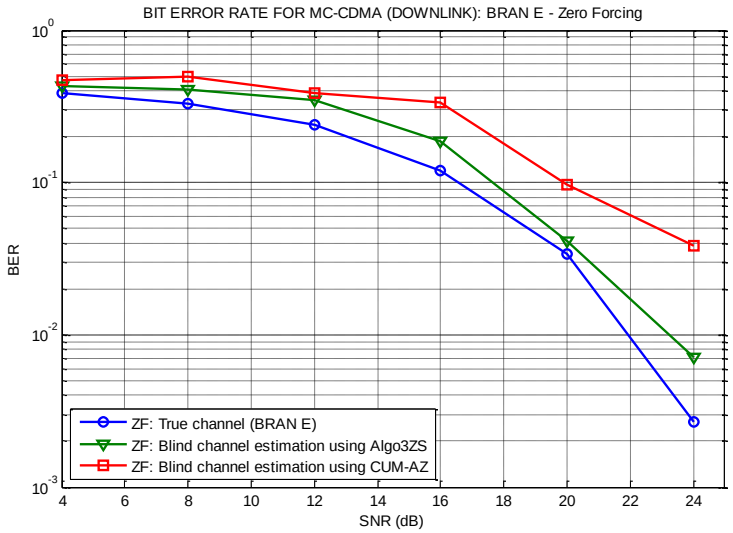

Figure 21. BER of the estimated and measured BRAN E channel using the ZF equalizer

Figure 22 represents the BER for different SNR, obtained using proposed algorithm (Algo3ZS), compared with the (CUM_AZ) algorithm, but the equalization is performed using the MMSE equalizer.

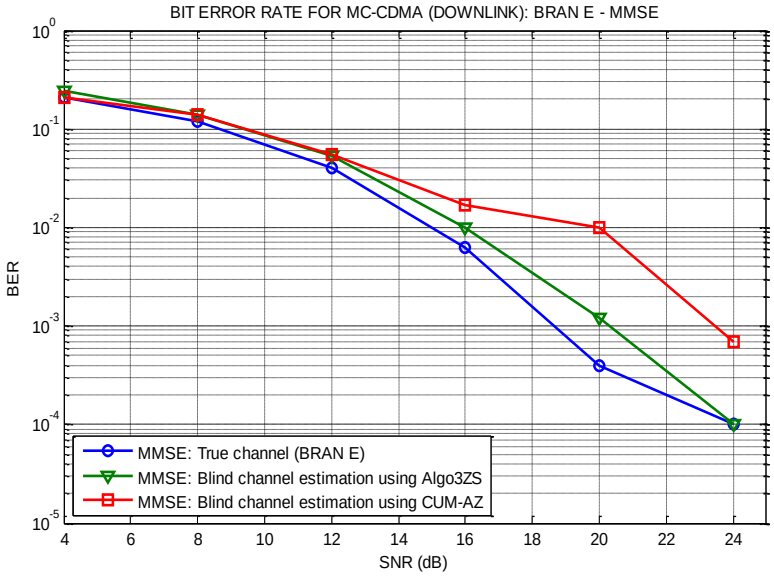

Figure 22. BER of the estimated and measured BRAN E channel using the MMSE equalizer

From the figure 22 we can conclude that the BER obtained using (Algo3ZS) gives a very good results like these obtained by (CUM_AZ). If the $SNR = 24\ dB$ we have a BER less than 10^{-3} using (Algo3ZS), but using the (CUM_AZ) we have only the BER less than 10^{-2}. In conclusion, for all channels the MMSE equalizer best than the ZF technique.

8. Conclusion

In this paper we have proposed an new algorithm (Algo3ZS) based on third order cumulants, compared with the Antari et al algorithm (CUM_AZ), to identify the parameters of the impulse response of the frequency selective channel such as the experimental channels, BRAN A, BRAN B, BRAN C, BRAN D, and BRAN E, normalized for MC-CDMA systems. The simulation results show the efficiency of the proposed algorithm (Algo3ZS) than those obtained using (CUM_AZ), mainly if the input data are sufficient. The magnitude and phase of the impulse response is estimated with an acceptable precision in noisy environment principally if we use the first algorithm (Algo3ZS). In part of five experimental channels for MC-CDMA systems application, we have obtained very important results on bit error rate using the proposed algorithm (Algo3ZS), than those obtained by (CUM_AZ) algorithm.

References

[1] G. B. Giannakis and A. Delopoulos, "cumulant based autocorrelation estimates of non-gaussian linear processes", Signal Processing, Elsevier, vol. 47, **(1995)**, pp. 1-17**.**

[2] J. M. Mendel, "tutorial on higher order statistics in signal processing and system theory: theoretical results and some applications", Procceeding of the IEEE, vol. 79, **(1991)**, pp. 278-305**.**

[3] C. L. Nikias and A. P. Petropulu, "higher order spectra analysis", PTR Prentice Hall, Englewood Cliffs, New Jersey, vol. 07632, **(1993).**
[4] S. Safi and A. Zeroual, "blind parametric identification of non-gaussian FIR systems using higher order cumulants", International Journal of Systems Science, vol. 35, **(2004)**, pp. 855-867**.**

[5] M. Zidane, S. Safi, M. Sabri and A. Boumezzough, "Impulse Response Identification of Minimum and Non Minimum Phase Channels", 4th Workshop on Codes, Cryptography and Communication Systems (WCCCS'13), **(2013)** November 07-08, Meknes, Morocco.
[6] J. Antari, R. Iqdour and A. Zeroual, "Forecasting the wind speed process using higher order statistics and fuzzy systems", Revue des Energies Renouvelables, vol. 9, **(2006)**, pp. 237-251**.**
[7] S. Safi, M. Frikel, M. M'Saad and A. Zeroual, "Blind Impulse Response Identification of frequency Radio Channels: Application to Bran A Channel", Int. J. Sig. Proces., vol. 4, **(2007)**, pp. 201-206**.**
[8] M. Zidane, S. Safi, M. Sabri and A. Boumezzough, "Blind Identification of Minimum Phase Channels Based On Higher Order Cumulants", International Conference on Intelligent Information and Network Technology (IC2INT'13), **(2013)** November 13-14, Settat, Morocco.
[9] M. Bakrim and D. Aboutajdine, "Cumulant-based identification of non gaussian moving average signals", Traitement du Signal, vol. 16, **(1999)**, pp. 175-186**.**
[10] J. Antari, A. El Khadimi, D. Mammas and A. Zeroual, "Developed Algorithm for Supervising Identification of Non Linear Systems using Higher Order Statistics: Modeling Internet Traffic", International Journal of Future Generation Communication and Networking, vol. 5, **(2012).**
[11] J. Antari, A. Zeroual and S. Safi, "Stochastic analysis and parametric identification of moving average (MA) non Gaussian signal using cumulants", International Journal of Physical and Chemical News, vol. 34, **(2007)**, pp. 27-32**.**
[12] S. Safi and A. Zeroual, "Blind identification in noisy environment of nonminimum phase finite impulse response (FIR) system using higher order statistics", vol. 43, **(2003)**, pp. 671-681**.**
[13] K. Abderrahim, R. B. Abdennour, G. favier, M. Ksouri and F. Msahli, "New results on FIR system identification using cumulants", APII-JESA, vol. 35, **(2001)**, pp. 601-622**.**
[14] ETSI, "Broadband Radio Access Networks (BRAN); High Performance Radio Logical Area Network (HIPERLAN) Type 2; Requirements and architectures for wireless broadband access", Janvier, **(1999).**
[15] ETSI, "Broadband Radio Access Networks (BRAN); HIPERLAN Type 2; Physical Layer", Decembre, **(2001).**
[16] S. Safi, "Identification aveugle des canaux à phase non minimale en utilisant les statistiques d'ordre supérieur: application aux réseaux mobiles", Thèse d'Habilité, Cadi Ayyad University, Marrakesh, Morocco, **(2008).**
[17] J. Antari, "analyse et identification aveugle des Systèmes non linéaire en utilisant les statistiques d'ordre, supérieur : application à la modélisation du trafic dans les réseaux internet", Thèse de Doctorat, Cadi Ayyad University, Marrakesh, Morocco, **(2008).**
[18] S. Safi and A. Zeroual, "Blind non-minimum phase channel identification using 3rd and 4th order cumulants", Int. J. Sig. Proces., vol. 4, **(2007)**, pp. 158-168**.**
[19] M. Frikel, B. Targui, M. M'Saad and F. Hamon, "Bit error rate analysis of the controlled equalization for MC-CDMA", in IEEE ICSPC'07 Conf., Dubai, United Arab Emirates, **(2007).**

